Journal of Inflammation Research

Dovepress
Taylor & Francis Group

Open Access Full Text Article

ORIGINAL RESEARCH

Establishment of a Novel in vitro Model of Sepsis-Induced Myocardial Injury Using Septic Serum: A Comprehensive Comparative Study

Hang Yang[1,*], Lin Feng[2,*], Zhenjie Jiang[1], Ruiming Deng[3], Xiaodan Wu[4], Kai Zeng[1]

[1]Department of Anesthesiology, Anesthesiology Research Institute, The First Affiliated Hospital of Fujian Medical University, Fuzhou, Fujian, People's Republic of China; [2]Department of Hematology, The First Affiliated Hospital of Fujian Medical University, Fuzhou, Fujian, People's Republic of China; [3]Department of Anesthesiology, Ganzhou People's Hospital, Ganzhou, Jiangxi, People's Republic of China; [4]Department of Anesthesiology, Shengli Clinical Medical College, Fujian Medical University, Fuzhou, Fujian, People's Republic of China

*These authors contributed equally to this work

Correspondence: Kai Zeng, Department of Anesthesiology, Anesthesiology Research Institute, The First Affiliated Hospital of Fujian Medical University, Fuzhou, Fujian, 350004, People's Republic of China, Email fymzk6822@163.com

Background: Sepsis is a life-threatening systemic inflammatory syndrome, in which myocardial injury plays a key role in disease progression and poor outcomes. However, the precise mechanisms underlying sepsis-induced myocardial injury remain unclear, and the most appropriate in vitro model for its investigation remains to be established. This study aimed to systematically compare different in vitro models to determine the most appropriate model for studying the pathophysiological mechanisms of sepsis-induced myocardial injury.

Materials and Methods: AC16 cardiomyocytes were treated with lipopolysaccharide (LPS), tumor necrosis factor-α (TNF-α), or septic serum for 24 hours to induce myocardial injury. Cell viability, cytotoxicity, inflammatory response, oxidative stress, apoptosis, and myocardial injury biomarkers were assessed to evaluate model performance. The mRNA expression profiles were analyzed to identify differentially expressed genes (DEGs), followed by functional enrichment analysis. The diagnostic utility of each model was assessed using receiver operating characteristic (ROC) analysis.

Results: While LPS and TNF-α-treated cardiomyocytes exhibited similar injury features, both only partially captured the complexity of the sepsis-induced myocardial injury phenotype. In contrast, cardiomyocytes exposed to septic serum demonstrated more pronounced inflammatory responses, oxidative stress, apoptosis, and myocardial damage. Transcriptomic analysis revealed that the septic serum model induced 706 DEGs, significantly more than LPS (262 DEGs) or TNF-α (237 DEGs), and enriched in a broader array of biological processes and signaling pathways. ROC analysis confirmed that the septic serum model (AUC=0.671, 0.610) had higher diagnostic accuracy for septic cardiomyopathy datasets compared to the LPS (AUC= 0.548, 0.426) and TNF-α (AUC= 0.470, 0.559) models.

Conclusion: This study introduces a novel in vitro approach using septic serum to model sepsis-induced myocardial injury, providing a physiologically relevant platform that more accurately reflects the complex pathophysiology of the disease.

Keywords: sepsis, myocardial injury, in vitro model, septic serum

Introduction

Sepsis is a life-threatening syndrome characterized by a dysregulated host response to infection, leading to multisystem organ dysfunction. It is a major cause of mortality and morbidity in intensive care units (ICUs) worldwide and imposes a substantial medical burden.[1–3] Among the various complications, sepsis-induced myocardial injury is particularly common and lethal. Approximately 60% of septic patients experience myocardial injury, with associated mortality rates reaching 70–90%.[4,5] Despite recent advances, the lack of effective diagnostic biomarkers and targeted therapies remains a significant challenge, largely due to an incomplete understanding of the underlying molecular mechanisms.

Received: 6 March 2025
Accepted: 13 June 2025
Published: 17 June 2025

To investigate the pathogenesis of sepsis-induced myocardial injury, the development of physiologically relevant and reliable in vitro models is essential. Currently, most studies utilize lipopolysaccharide (LPS) to induce inflammatory injury in cardiomyocytes and simulate the immune response associated with sepsis.[6–8] LPS activates Toll-like receptor 4 (TLR4), triggering downstream inflammatory cascades, excessive cytokine release, oxidative stress, and ultimately cardiomyocyte dysfunction.[9–12] While LPS-based models partially reproduce the inflammatory milieu of sepsis, they fail to reflect the systemic immune, metabolic, and neurohumoral alterations observed in clinical settings.[13–15] Similarly, tumor necrosis factor-α (TNF-α), a key proinflammatory cytokine in sepsis, promotes cardiomyocyte apoptosis, mitochondrial dysfunction, and impaired contractility through activation of NF-κB and other downstream pathways.[16,17] However, as with LPS, single-factor stimulation cannot replicate the complex biological environment of sepsis, which involves multiple cytokines, chemokines, and damage-associated molecular patterns acting in concert. Therefore, standardized and comprehensive in vitro models of sepsis-induced myocardial injury are still lacking. Finding a suitable in vitro model of sepsis-induced myocardial injury is crucial to explore the mechanism of sepsis-induced myocardial injury.

To address these limitations, we investigated the use of septic serum, which contains a dynamic and physiologically relevant mixture of inflammatory mediators, endotoxins, metabolic by-products, and immune components that better reflect the multifaceted pathophysiology of sepsis.[18–20] Septic serum may thus offer a more accurate and clinically relevant model of sepsis-induced myocardial injury.

In this study, we established in vitro models of sepsis-induced myocardial injury by treating cardiomyocytes with LPS, TNF-α, and septic serum. By assessing a range of cellular responses, including cell viability, cytotoxicity, inflammatory cytokine production, oxidative stress, apoptosis and myocardial injury markers, as well as performing transcriptomic profiling, we aimed to identify the most suitable model. Our findings provide a foundation for future mechanistic studies and the development of targeted therapeutic strategies for sepsis-induced myocardial injury.

Materials and Methods

Acquisition of Septic Serum

Healthy adult male C57BL/6J mice (weighing 25 ± 3 g) were randomly divided into two groups: a sham group (n=10) and a sepsis group (n=10). All procedures involving animals complied with the Guide for the Care and Use of Laboratory Animals (National Research Council, 2011) and were approved by the Fujian Medical University Institutional Animal Care and Use Committee (FJMU IACUC 2021–0336). LPS (Sigma, L2880, USA) was dissolved in normal saline at a concentration of 3 mg/mL, and 0.1 mL of this solution was administered intraperitoneally to each mouse in the sepsis group, a dose previously shown to induce systemic inflammation and cardiac injury.[21–23] The sham group received an intraperitoneal injection of an equivalent volume of normal saline. Cardiac structure and function were evaluated 24 hours after LPS injection (see Figure S1). Successful establishment of the sepsis-induced myocardial injury model was confirmed by the presence of typical systemic symptoms, such as decreased activity, hypothermia, and listlessness, along with evidence of cardiac structural and functional impairment consistent with established criteria. After establishing the sepsis-induced myocardial injury model, blood was collected immediately. Serum from ten mice per group was pooled to minimize individual variability, centrifuged to remove cellular debris, filtered, and stored at −80 °C for subsequent experiments. Control serum was similarly obtained from sham-operated mice and processed in parallel.

All invasive procedures were performed under anesthesia using isoflurane with oxygen. Buprenorphine (0.1 mg/kg, subcutaneous injection) was administered to relieve pain and minimize distress. To ensure animal welfare, mice were maintained on a heated pad during procedures and continuously monitored for signs of pain, distress, or abnormal behavior over the 24-hour observation period. Humane endpoints included severe hypothermia, profound lethargy, or unresponsiveness to stimuli. Animals meeting these criteria were euthanized immediately according to the AVMA Guidelines for the Euthanasia of Animals (2020), using an overdose of sodium pentobarbital. All personnel involved in animal care were specially trained in the use of anesthesia, analgesia, and animal monitoring techniques to ensure compliance with ethical guidelines and improve data reliability.[24] A total of 26 mice were included in this study. Of these, 20 mice were euthanized according to humane endpoints, while 6 mice died prior to meeting euthanasia criteria.

Postmortem examination determined that their deaths were caused by multiple organ damage resulting from an excessive inflammatory response.

In vitro Model Construction

AC16 cardiomyocytes (Pricella, CL-0790) were cultured in Dulbecco's Modified Eagle Medium (DMEM) supplemented with 10% fetal bovine serum (FBS) and 1% penicillin-streptomycin. Cells at passages 4–8 were used in all experiments. The control group received no treatment. To establish an in vitro model of sepsis-induced myocardial injury, cells were treated for 24 hours with either LPS (10 μg/mL; Sigma, L2880, USA), TNF-α (1 ng/mL; Pricella, PCK050, China), or septic serum (10 μL/mL) in the LPS, TNF-α, and serum groups, respectively. These concentrations were selected based on previous publications and preliminary experiments, which demonstrated that they effectively induce cardiomyocyte injury without causing excessive cytotoxicity.[25,26] A 24-hour treatment duration was chosen because it captures key cellular responses, including inflammatory activation and early markers of myocardial injury, while minimizing late-stage or nonspecific effects. The experimental scheme is illustrated in Figure 1. All experiments were conducted independently at least three times using biological replicates.

Enzyme-Linked Immunosorbent Assay (ELISA)

ELISA kits were used to quantify the levels of Interleukin-1β (IL-1β) (Boster, EK0394, China), Interleukin-6 (IL-6) (Boster, EK0411, China) and Tumor necrosis factor-α (TNF-α) (Boster, EK0527, China) in mouse serum. In addition, culture supernatants were collected after 24 hours of treatment by centrifuging the media at 1000 × g for 5 minutes, followed by storage at −80 °C until cytokine analysis. ELISA kits were also employed to detect markers of myocardial injury in the cell supernatant, including brain natriuretic peptide (BNP) (Elabscience, E-EL-H6166, China), creatine kinase-MB (CK-MB) (CUSABIO, CSB-E05140h, China), and cardiac troponin I (cTnI) (CUSABIO, CSB-E05139h, China). All procedures were performed strictly in accordance with the manufacturers' instructions. Cytokine and biomarker concentrations were normalized using standard reagents provided with each kit.

Hematoxylin-Eosin (HE) Staining

Ventricular myocardium was harvested from mice and immediately fixed in 4% paraformaldehyde at room temperature for 24 hours. The fixed tissue was subsequently dehydrated through a graded ethanol series, cleared in xylene, and embedded in paraffin. Serial sections of 5 μm thickness were cut using a microtome and mounted onto glass slides. Sections were dewaxed, rehydrated, stained with hematoxylin for 5 minutes, followed by brief rinsing in distilled water and differentiation in acid alcohol. After counterstaining with eosin for 2 minutes, the slides were dehydrated, cleaned,

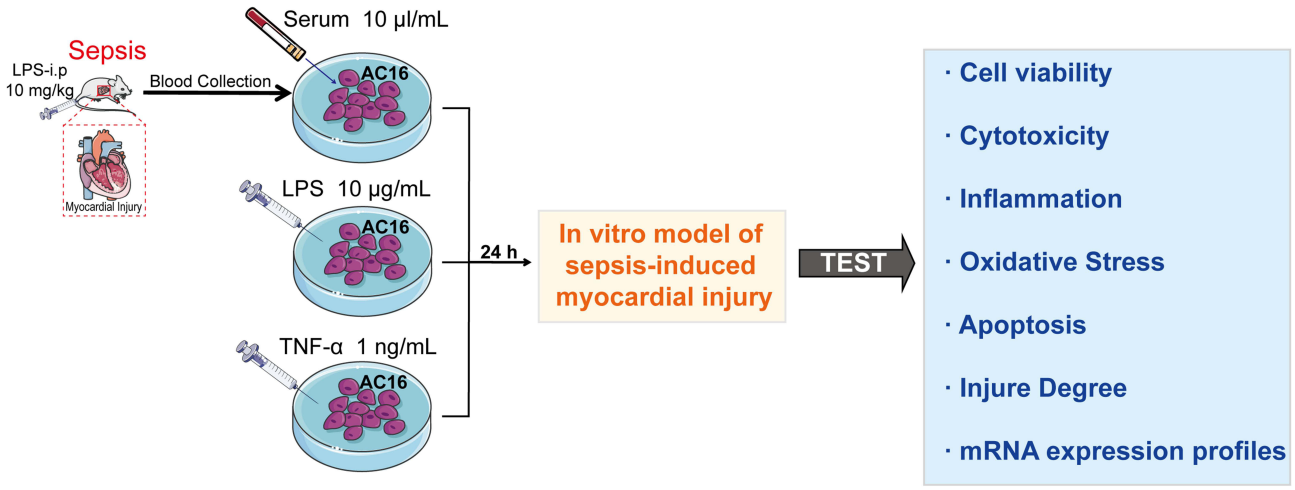

Figure 1 The flowchart of this study.
Abbreviations: i.p, intraperitoneal; LPS, Lipopolysaccharide; TNF-α, Tumor necrosis factor-α.

https://doi.org/10.2147/JIR.S523124

and mounted with neutral resin. Histopathological alterations in myocardial tissue, including inflammatory cell infiltration, myocyte swelling, and disruption of structural integrity, were observed under a light microscope (Leica, RM2235, Germany).

Echocardiographic Examination

Mice were anesthetized using a mixture of isoflurane and oxygen, and anesthesia was confirmed prior to examination. Cardiac function was assessed using transthoracic echocardiography (Youkey, Guangdong, China). M-mode imaging was used to measure the left ventricular internal diameter at end-diastole (LVIDd) and at end-systole (LVIDs). Left ventricular ejection fraction (LVEF) and left ventricular fractional shortening (LVFS) were subsequently calculated based on these dimensions. To ensure consistency, all echocardiographic assessments were conducted by the same operator. Each parameter was measured in triplicate for each mouse to ensure accuracy and reproducibility.

Electrocardiograph (ECG) Monitoring

After anesthetizing the mice, electrodes were attached to each limb in accordance with the standard lead configuration. A stable lead II electrocardiogram (ECG) was continuously recorded for 5 minutes using the MD3000 biological signal acquisition and processing system (Zhenghua Bioinstrument, Huaibei, China). Care was taken to minimize movement and external disturbances to ensure accurate and artifact-free ECG data acquisition.

Cell Counting Kit-8 (CCK8)

Cell viability was assessed using the CCK-8 assay (Elabscience, E-CK-A362, China). Cardiomyocytes were seeded into 96-well plates at a density of 5×10^4 cells per well and incubated overnight. Following 24 hours of treatment, 10 μL of CCK-8 reagent was added to each well, and the plates were incubated at 37 °C in a humidified atmosphere containing 5% CO_2 for 2 hours. The absorbance at 450 nm was then measured using a microplate reader (Tecan, Infinite M PLEX, Switzerland). Cell viability was expressed as a percentage relative to the untreated control group.

Lactatedehydrogenase (LDH) Release Assay

LDH release was measured using an LDH detection kit (Jiangcheng, Nanjing, A020-2-1, China) to evaluate cell membrane integrity. Following 24 hours of treatment, 100 μL of culture supernatant was collected from each well and transferred to a 96-well plate. Subsequently, 50 μL of LDH detection reagent was added to each well, and the plate was incubated at 37 °C in the dark for 30 minutes. Absorbance was measured at 490 nm using a microplate reader (Tecan, Infinite M PLEX, Switzerland). The percentage of LDH release was calculated to reflect the extent of cytotoxicity.

Reverse Transcription Quantitative Polymerase Chain Reaction (RT-qPCR)

Total RNA was extracted from each group of cells (1×10^5 cells/well) using an RNA extraction kit (Beyotime, R0017M, China). Complementary DNA (cDNA) was synthesized using a reverse transcription kit (Beyotime, D7170M, China) according to the manufacturer's instructions. qRT-PCR was performed using the ChamQ Universal SYBR qPCR Master Kit (Vazyme, Q711-02, China). The thermal cycling conditions were as follows: initial denaturation at 95 °C for 30 seconds, followed by 40 cycles of 95 °C for 5 seconds and 60 °C for 30 seconds. A melting curve analysis was conducted at the end of the amplification cycles to verify the specificity of the products. GAPDH was used as the internal control gene. Relative mRNA expression levels were calculated using the $2^{\wedge-\Delta\Delta CT}$ method. Primer sequences are listed in Table S1.

Cell Bioenergetic Tests

AC16 cardiomyocytes were seeded into an XF96 cell culture microplate, and subjected to bioenergetic analysis after 24 hours of treatment. Prior to the assay, cells were washed twice with seahorse assay medium and incubated in a non-CO_2 incubator at 37 °C for 1 hour to allow for pH and temperature equilibration. The oxygen consumption rate (OCR) reagents were loaded into the appropriate ports of the sensor cartridge, which was then calibrated using the Seahorse

XFe96 Analyzer (Agilent Technologies, USA). Upon successful calibration, the cell culture plate was loaded into the analyzer, and real-time measurements of OCR were recorded.

Reactive Oxygen Species (ROS) Assay Assessment

After 24 hours of treatment, cells in each group were washed with serum-free medium, followed by incubation with 10 μmol/L DCFH-DA fluorescent probe at 37 °C for 30 minutes in the dark. After incubation, cells were washed again to remove excess probe. ROS levels were then visualized and captured using a fluorescence microscope. Quantification of fluorescence intensity was performed using ImageJ software.

Flow Cytometry (FCM)

Apoptosis in AC16 cardiomyocytes was evaluated using flow cytometry. Briefly, 1×10^6 cells from each group were seeded in 6-well plates and treated for 24 hours. Following treatment, cells were harvested, washed twice with PBS, and stained with Annexin V-FITC (Beyotime, C1062S, China) according to the manufacturer's instructions. The cells were incubated in the dark at room temperature for 15 minutes, and apoptotic populations were subsequently analyzed using a flow cytometer.

Tunel Staining

Following treatment, cells in each group were washed twice with PBS and fixed with 4% paraformaldehyde for 30 minutes. The TUNEL kit (Elabscience, E-CK-A321, China) was used to detect apoptosis rate, according to the manufacturer's instructions. TUNEL-positive staining was observed, and the apoptosis rate was calculated.

Identification and Functional Enrichment Analysis of Differentially Expressed Genes (DEGs)

Transcriptomic analysis was performed to assess mRNA expression profiles across experimental groups, including three samples each from the control, LPS, TNF-α, and serum-treated groups (Table S2). The "Limma-voom" R package was used to analyze the DEGs. The DEGs with |log2 fold change (FC)| >0.583 and P value < 0.05 were considered statistically significant. Heatmaps and volcano plots of DEGs were generated using the "Pheatmap" and "ggplot2" R packages, respectively. Gene Ontology (GO) and Kyoto Encyclopedia of Genes and Genomes (KEGG) pathway analyses were conducted using the "clusterProfiler" R package to evaluate biological processes (BP), molecular functions (MF), cellular components (CC), and signaling pathways. GO terms and KEGG pathways with P values < 0.05 were deemed significantly enriched.

Evaluation of the Diagnostic Value

Septic cardiomyopathy datasets (GSE79962 and GSE237861) were obtained from Gene Expression Omnibus (GEO) database (https://www.ncbi.nlm.nih.gov/geo/). Data were transformed using transcripts per million (TPM), averaged, normalized, and log-normalized [log(TPM+1)]. Gene set variation analysis (GSVA) was performed on the DEGs in the in vitro model of sepsis-induced myocardial injury treated with LPS, TNF-α, and septic serum in GSE79962 and GSE237861 datasets, respectively, and the GSVA score was calculated. Then, receiver operating characteristic curves (ROC) were plotted to evaluate the diagnostic value of DEGs in each group of sepsis-induced myocardial injury in vitro models for sepsis-induced myocardial injury.

Statistical Analysis

Statistical analyses were conducted using SPSS software (version 26.0) and R software (version 4.2.0). All data were presented as the mean ± standard deviation. One-way analysis of variance (ANOVA) was used to compare differences among multiple groups, followed by the least significant difference (LSD) method for pairwise comparisons. The Student's t-test was applied for comparisons between two groups. The Grubbs test was used to detect outliers, and no

data points were excluded from the final analysis. Data were assessed for normality using the Shapiro–Wilk test, with appropriate transformations applied if necessary. A p-value of less than 0.05 was considered statistically significant.

Results

Inflammatory Responses in Various in vitro Models of Sepsis-Induced Myocardial Injury

To evaluate the inflammatory response, we measured the expression levels of pro-inflammatory and anti-inflammatory genes in each group. Compared to the control group [IL-6 (1.01± 0.13); IL-1β (1.00 ± 0.07)], IL-6 and IL-1β expression was significantly upregulated in the LPS [IL-6 (1.34 ± 0.10); IL-1β (2.04 ± 0.15)], TNF-α [IL-6 (1.70 ± 0.08); IL-1β (2.69 ± 0.58)], and serum [IL-6 (1.93 ± 0.13); IL-1β (3.91 ± 0.88)] groups (P<0.05). IL-6 expression in the TNF-α group was significantly higher than in the LPS group (P<0.01), whereas no significant difference in IL-1β expression was observed between these two groups (P>0.05). Notably, both IL-6 and IL-1β expression levels were significantly higher in the serum group than in the LPS and TNF-α groups (P<0.05) (Figure 2A and B). Additionally, the expression of the anti-inflammatory gene TGF-β was significantly reduced in the LPS (0.55 ± 0.07), TNF-α (0.60 ± 0.09), and serum (0.57 ± 0.13) groups compared to the control group (1.02 ± 0.23) (P < 0.01), with no significant differences among the three treatment groups (P > 0.05) (Figure 2C). There were no significant differences in IL-10 expression among the control (1.02 ± 0.23), LPS (0.98 ± 0.22), and TNF-α (0.78 ± 0.01) groups (P>0.05). However, IL-10 expression was significantly lower in the serum group (0.44 ± 0.02) compared to the control, LPS, and TNF-α groups (P < 0.05) (Figure 2D). These findings suggest that the in vitro model of sepsis-induced myocardial injury established using septic serum effectively replicates the inflammatory milieu of sepsis in cardiomyocytes, including alterations in both pro-inflammatory and anti-inflammatory mediators.

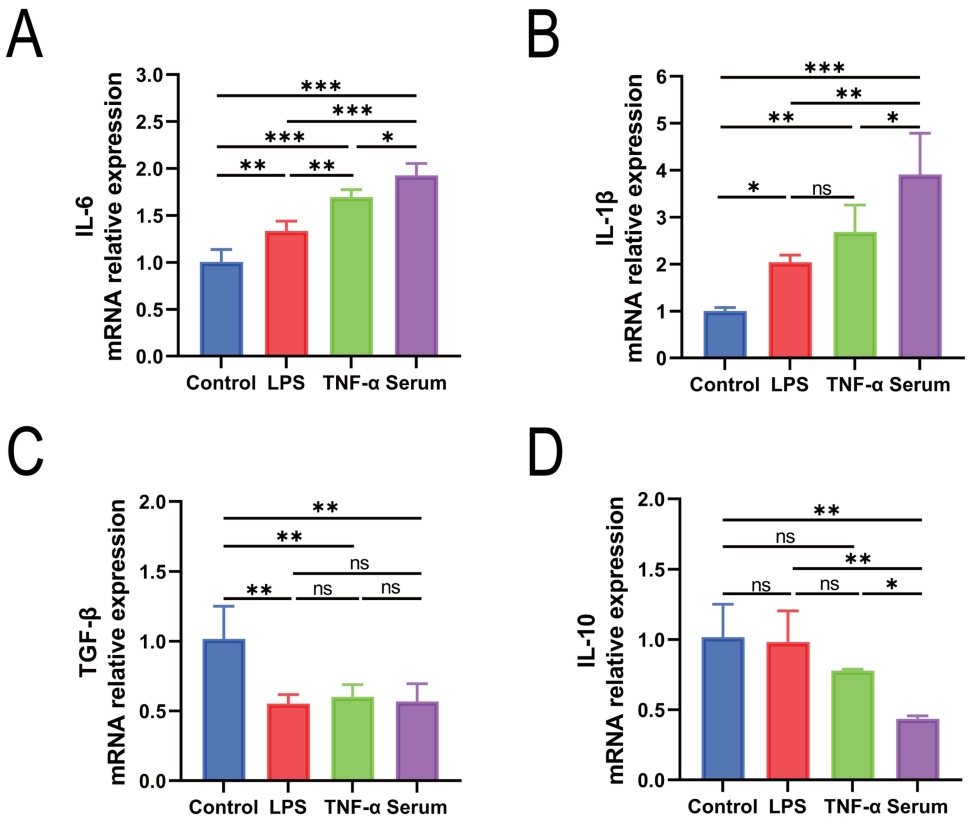

Figure 2 Comparison of inflammatory responses in various in vitro models of sepsis-induced myocardial injury. (**A**–**D**) The expression levels of IL-6, IL-1β, TGF-β and IL-10 in each group. *P < 0.05, **P < 0.01, ***P < 0.001.

Abbreviations: LPS, Lipopolysaccharide; TNF-α, Tumor necrosis factor-α; IL-6, Interleukin-6; IL-1β, Interleukin-1β; TGF-β, Transforming growth factor-β; IL-10, Interleukin-10; ns, not significant.

Oxidative Stress in Various in vitro Models of Sepsis-Induced Myocardial Injury

Mitochondrial function and ROS levels were assessed to evaluate oxidative stress. As shown in Figure 3A, OCR measurements revealed that basal respiration was significantly reduced in the LPS (50.24 ± 5.34 pmol/min), TNF-α (47.31 ± 5.95 pmol/min), and serum (38.54 ± 6.25 pmol/min) groups compared to the control group (56.32 ± 2.91 pmol/min) ($P<0.05$). No significant difference was observed between the LPS and TNF-α groups ($P>0.05$), while basal respiration in the serum group was significantly lower than in both the LPS and TNF-α groups ($P<0.01$) (Figure 3B). ATP production was not significantly altered in the LPS (51.63 ± 3.74 pmol/min) or TNF-α (49.75 ± 4.64 pmol/min) groups compared to the control group (53.38 ± 5.85 pmol/min) ($P > 0.05$). However, the serum group showed a marked reduction in ATP production (34.91 ± 6.78 pmol/min) ($P < 0.001$) (Figure 3C). Maximal respiratory capacity was also significantly decreased in the LPS (74.16 ± 6.73 pmol/min), TNF-α (63.90 ± 5.06 pmol/min), and serum (46.17 ± 5.25 pmol/min) groups compared to the control group (107.57 ± 1.45 pmol/min) ($P < 0.001$), with the serum group exhibiting a significantly greater reduction than the other two groups ($P < 0.001$) (Figure 3D). Similarly, spare respiratory capacity was markedly decreased in the LPS (23.92 ± 5.58 pmol/min), TNF-α (16.59 ± 3.84 pmol/min), and serum (7.64 ± 2.85 pmol/min) groups relative to the control group (51.24 ± 2.96 pmol/min) ($P < 0.001$), and this reduction was most pronounced in the serum group ($P < 0.001$) (Figure 3E).

ROS detection revealed no significant difference in ROS levels among the control (0.05 ± 0.03%), LPS (0.04 ± 0.02%), and TNF-α (0.05 ± 0.02%) groups ($P > 0.05$). In contrast, ROS levels in the serum group (0.11 ± 0.03%) were significantly higher than in the other three groups ($P < 0.05$) (Figure 3F).

These results indicate that septic serum treatment induces a more severe impairment of mitochondrial function and a greater degree of oxidative stress in cardiomyocytes compared to LPS or TNF-α stimulation alone.

Apoptotic Rates in Various in vitro Models of Sepsis-Induced Myocardial Injury

Apoptosis levels in cardiomyocytes were assessed to evaluate cellular damage induced by different modeling approaches. Flow cytometry analysis revealed that, compared to the control group (8.89 ± 0.23%), apoptosis rates were significantly increased in the LPS (19.09 ± 0.30%), TNF-α (22.50 ± 0.48%), and serum groups (23.48 ± 0.08%) ($P<0.001$). Notably, the serum group exhibited a significantly higher apoptosis rate than both the LPS group and TNF-α groups ($P<0.001$) (Figure 4A). Consistently, TUNEL staining revealed increased apoptotic areas in the LPS (0.05 ± 0.01%), TNF-α (0.07 ± 0.01%), and serum (0.25 ± 0.01%) groups compared to the control group (0.02 ± 0.01%) ($P < 0.05$). The apoptotic area was markedly higher in the serum group than in the LPS and TNF-α groups ($P < 0.001$), while no significant difference was observed between the LPS and TNF-α groups ($P > 0.05$) (Figure 4B). These findings suggest that septic serum induces a greater degree of cardiomyocyte apoptosis than LPS or TNF-α, highlighting the potential severity of systemic factors present in septic serum. However, the underlying molecular pathways responsible for this increased apoptosis warrant further investigation.

Degree of Myocardial Injury in Various in vitro Models of Sepsis-Induced Myocardial Injury

The optimal concentrations of LPS, TNF-α, and septic serum for inducing cardiomyocyte injury were determined to be 10 μg/mL, 1 ng/mL, and 10 μL/mL, respectively (Figure 5A–C). At these optimal concentrations, cell viability was significantly reduced in the LPS (0.49 ± 0.02), TNF-α (0.44 ± 0.06), and serum (0.29 ± 0.02) groups compared to the control group. Notably, the decrease in cell viability was significantly greater in the serum group than in the LPS and TNF-α groups ($P < 0.001$) (Figure 5D). Correspondingly, LDH release in the supernatant, a marker of cell membrane damage, was elevated in the LPS (318.02 ± 60.89 U/L), TNF-α (353.09 ± 58.56 U/L), and serum (451.85 ± 52.58 U/L) groups, compared to the control group (181.23 ± 37.14 U/L) ($P < 0.01$). Although there was no significant difference in LDH levels between the LPS and TNF-α groups ($P > 0.05$), LDH release was significantly higher in the serum group than in either the LPS or TNF-α group ($P < 0.05$) (Figure 5E).

To directly assess myocardial injury, we further examined key myocardial injury biomarkers in each group. There was no significant difference in BNP levels between the control (176.53 ± 8.30 pg/mL) and LPS (185.40 ± 12.78 pg/mL) groups ($P > 0.05$). However, BNP levels were significantly elevated in the TNF-α (238.14 ± 9.09 pg/mL) and serum (343.83 ± 37.27 pg/mL) groups compared to the control, with the serum group also showing significantly higher BNP levels than the TNF-α group ($P < 0.05$) (Figure 5F). Similarly, cTnI levels were markedly increased in the LPS (136.80 ± 4.37 pg/mL), TNF-α (168.80 ± 14.79 pg/

https://doi.org/10.2147/JIR.S523124

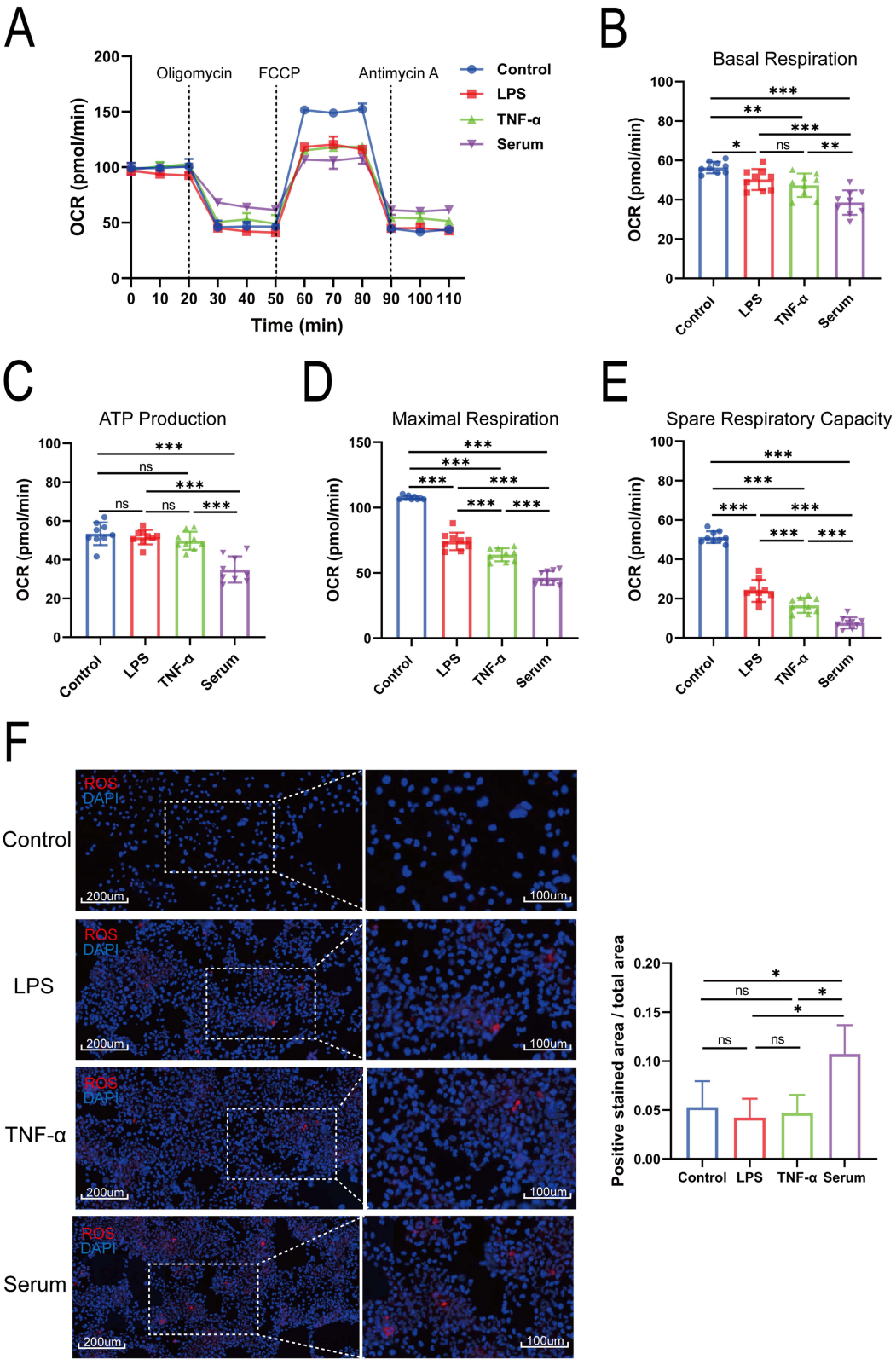

Figure 3 Comparison of oxidative stress responses in various in vitro models of sepsis-induced myocardial injury. (**A**–**E**) OCR for each group, as well as basal respiration, ATP production, maximal respiration, and spare respiratory capacity. (**F**) ROS levels in each group. *P < 0.05, **P < 0.01, ***P < 0.001.
Abbreviations: LPS, Lipopolysaccharide; TNF-α, Tumor necrosis factor-α; OCR, Oxygen consumption rate; ROS, Reactive oxygen species; ns, not significant.

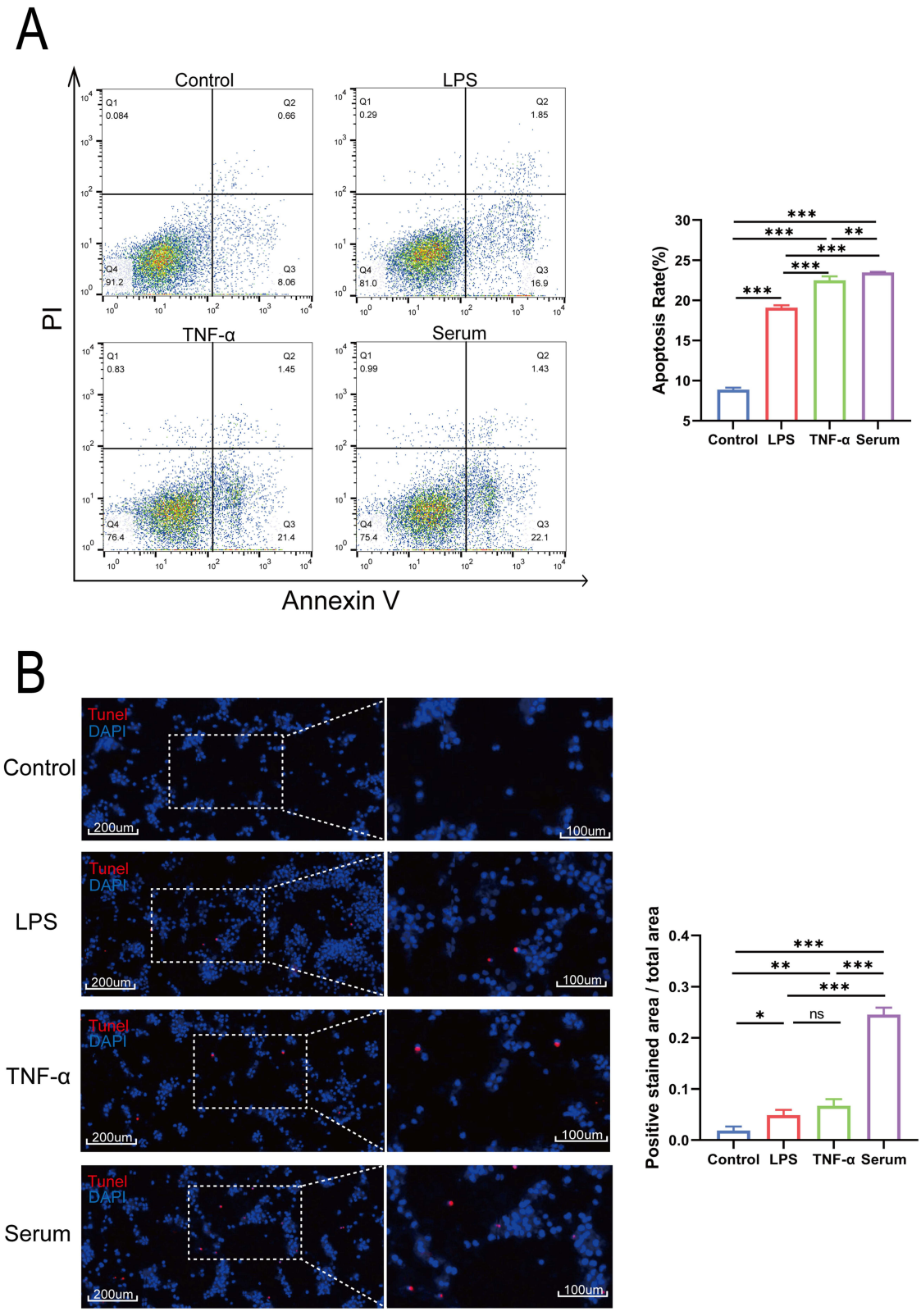

Figure 4 Comparison of apoptosis rates in various in vitro models of sepsis-induced myocardial injury. (**A** and **B**) The apoptosis level of each group. **P* < 0.05, ***P* < 0.01, ****P* < 0.001.

Abbreviations: LPS, Lipopolysaccharide; TNF-α, Tumor necrosis factor-α; ns, not significant.

https://doi.org/10.2147/JIR.S523124

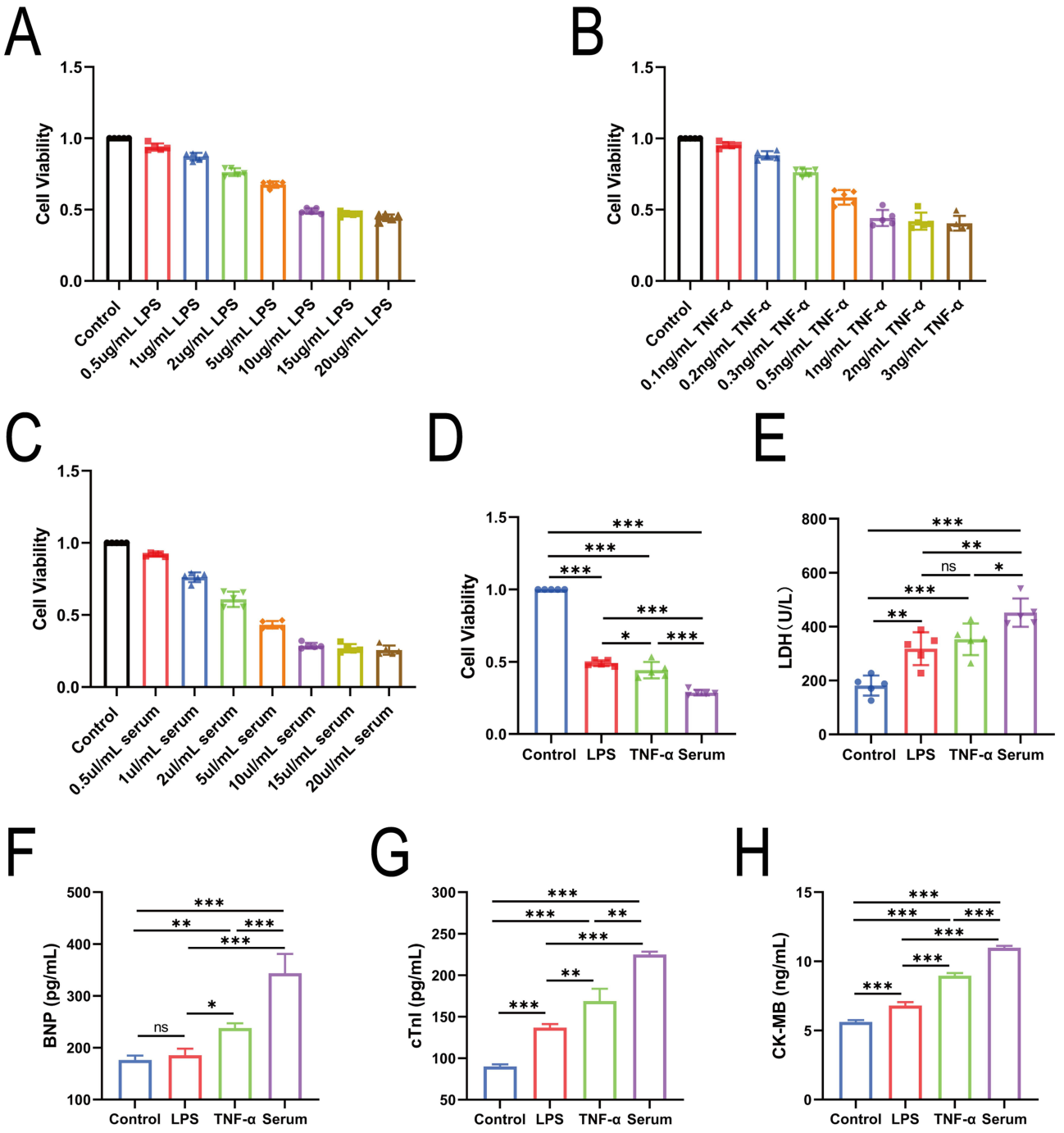

Figure 5 Comparison of the degree of injury in various in vitro models of sepsis-induced myocardial injury. (**A**–**D**) Cell viability of cardiomyocytes treated with LPS, TNF-α and septic serum. (**E**) LDH release level in each group. (**F**–**H**) The levels of BNP, cTnI and CK-MB in the supernatant of each group. *$P < 0.05$, **$P < 0.01$, ***$P < 0.001$.
Abbreviations: LPS, Lipopolysaccharide; TNF-α, Tumor necrosis factor-α; BNP, Brain natriuretic peptide; cTnI, cardiac troponin I; CK-MB, CreatineKinase-MB; ns, not significant.

mL), and serum (224.88 ± 3.45 pg/mL) groups compared to the control (90.16 ± 2.51 pg/mL), with the highest levels observed in the serum group ($P < 0.001$) (Figure 5G). CK-MB levels followed a similar trend, with significant increases observed in the LPS (6.80 ± 0.24 ng/mL), TNF-α (8.96 ± 0.19 ng/mL), and serum (10.98 ± 0.14 ng/mL) groups compared to the control (5.61 ± 0.14 ng/mL), and with the serum group showing significantly higher CK-MB levels than both the LPS and TNF-α groups ($P < 0.001$) (Figure 5H).

In summary, septic serum treatment resulted in more pronounced reductions in cardiomyocyte viability and greater elevations in injury biomarkers than LPS or TNF-α treatment, suggesting that this model more accurately recapitulates the pathophysiological features of sepsis-induced myocardial injury observed in clinical settings.

DEGs and Functional Enrichment Pathways in Various in vitro Sepsis-Induced Myocardial Injury Models

A total of 262 DEGs were identified in the LPS group, comprising 203 upregulated and 59 downregulated genes. In the TNF-α group, 237 DEGs were detected, including 195 upregulated and 42 downregulated genes. The serum group exhibited a markedly larger number of DEGs, totaling 706, with 664 upregulated and 42 downregulated genes (Figure 6A and B, Table S3). This broader transcriptional response in the serum group suggests that the septic serum model may more comprehensively reflect the gene expression alterations associated with sepsis, although the number of DEGs alone does not fully determine the fidelity of the model. Notably, analysis of the GSE79962 and GSE23781 datasets revealed that the serum group demonstrated greater diagnostic value for sepsis-induced cardiomyopathy compared to the LPS and TNF-α groups (Figure 6C).

GO enrichment analysis revealed distinct biological processes among the three groups (Figure 7). In the LPS group, DEGs were primarily enriched in "ribonucleoprotein complex biogenesis", "catalytic activity, acting on a nucleic acid", "establishment of protein localization to the endoplasmic reticulum", and "protein targeting to the ER" (Figure 7A). In the TNF-α group, enriched terms included "DNA repair", "chromosome organization", "antigen processing and presentation of endogenous peptide antigen via MHC class I", and related processes (Figure 7B). DEGs in the serum group were mainly associated with "chromosomal region", "cell division", "negative regulation of mitochondrial membrane permeability", and "negative regulation of mitochondrial outer membrane permeabilization involved in apoptotic signaling" (Figure 7C and Table S4).

Similarly, KEGG pathway analysis identified distinct signaling pathways enriched in each group (Figure 8). In the LPS group, significant pathways included "mitophagy-animal", "fatty acid elongation", "antigen processing and presentation", and the "insulin signaling pathway" (Figure 8A). DEGs in the TNF-α group were enriched in pathways such as "basal transcription factors", "non-homologous end-joining", "primary immunodeficiency" and "parathyroid hormone synthesis, secretion, and action" (Figure 8B). In contrast, the serum group showed enrichment in "cell cycle", "homologous recombination", "cGMP-PKG signaling pathway", and "cellular senescence" pathways (Figure 8C and Table S5).

Discussion

By comprehensively comparing inflammatory response, oxidative stress, myocardial injury, apoptosis, and gene expression across various in vitro models of sepsis-induced myocardial injury induced by LPS, TNF-α, and septic serum, we found that septic serum was the most effective inducer and could most comprehensively recapitulate the pathological features of septic myocardial injury. This model reflects a multifactorial injury mechanism, underscoring its potential as a more representative in vitro model.

The pathogenesis of sepsis-induced myocardial injury is complex and closely related to excessive inflammatory response, oxidative stress, apoptosis, and other mechanisms.[27–31] Inflammatory is a hallmark of organ dysfunction in sepsis, particularly within the cardiovascular system.[32] Consistent with previous studies, both LPS and TNF-α induced increased production of pro-inflammatory cytokines without significantly affecting anti-inflammatory cytokines in cardiomyocytes, thus failing to replicate the multifaceted immune interactions observed clinically.[33] In contrast, treatment with septic serum not only enhanced pro-inflammatory cytokine expression but also suppressed anti-inflammatory cytokines, eliciting a more pronounced inflammatory response. This suggests that septic serum contains a broader array of cytokines, chemokines, and immune mediators, more accurately reflecting the dysregulated immune state characteristic of clinical sepsis. These findings highlight mechanistic differences from single-agent models. The imbalance between pro- and anti-inflammatory factors may exacerbate myocardial injury by sustaining inflammation, warranting further exploration into the downstream signaling pathways that mediate this dual effect.

Oxidative stress in sepsis leads to excessive production of ROS, which impair mitochondrial function and promote apoptosis, ultimately contributing to myocardial injury.[6,34,35] We observed that septic serum markedly increased ROS

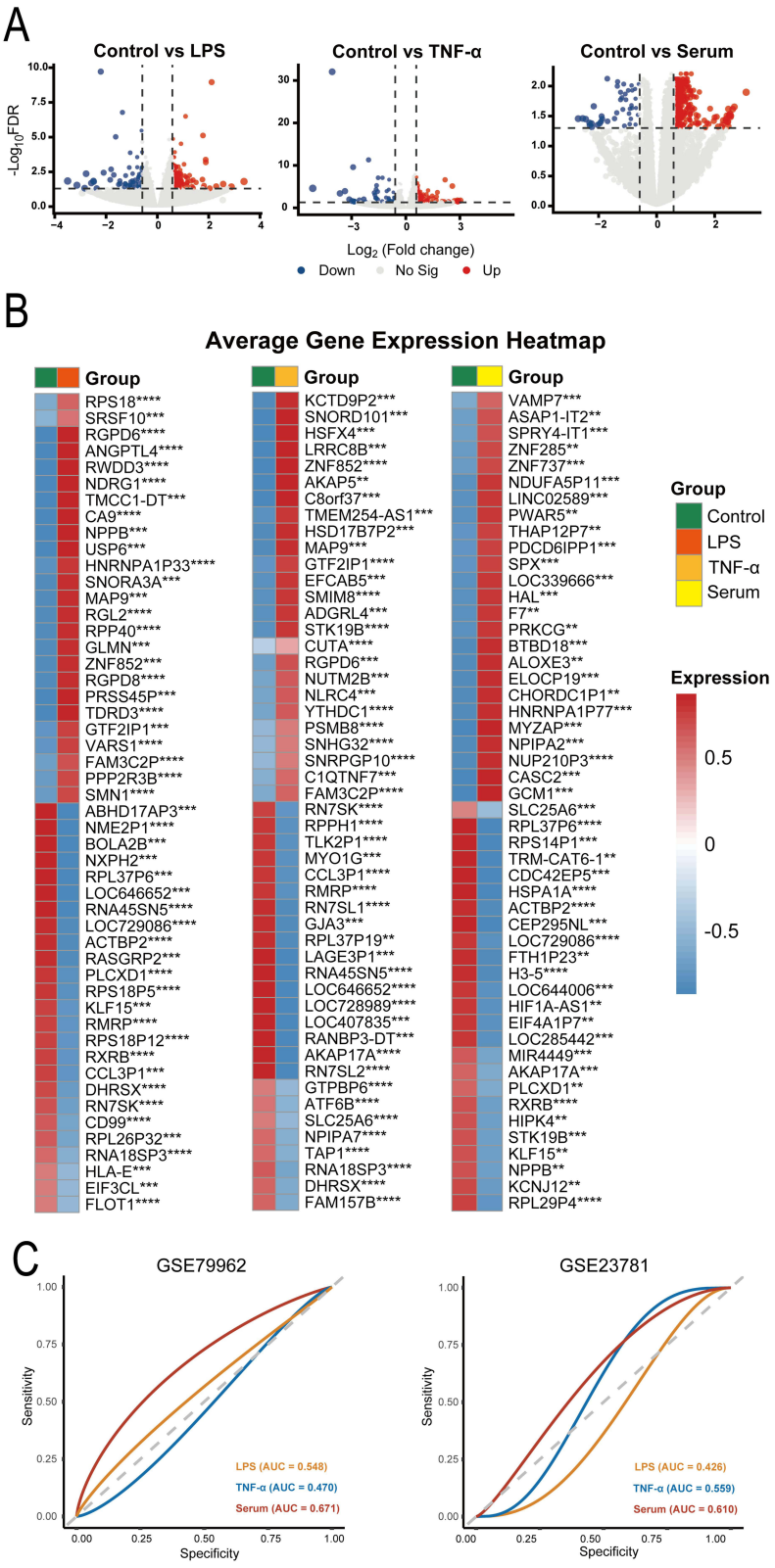

Figure 6 Differentially expressed genes (DEGs) in various in vitro models of sepsis-induced myocardial injury. (**A**) Volcano plots of DEGs in each group. (**B**) Heatmaps of DEGs in each group. (**C**) Evaluation of the diagnostic value of DEGs in the septic cardiomyopathy datasets (GSE79962 and GSE23781). **P* < 0.05, ***P* < 0.01, ****P* < 0.001, *****P* < 0.0001.

Abbreviations: LPS, Lipopolysaccharide; TNF-α, Tumor necrosis factor-α; AUC, area under the curve.

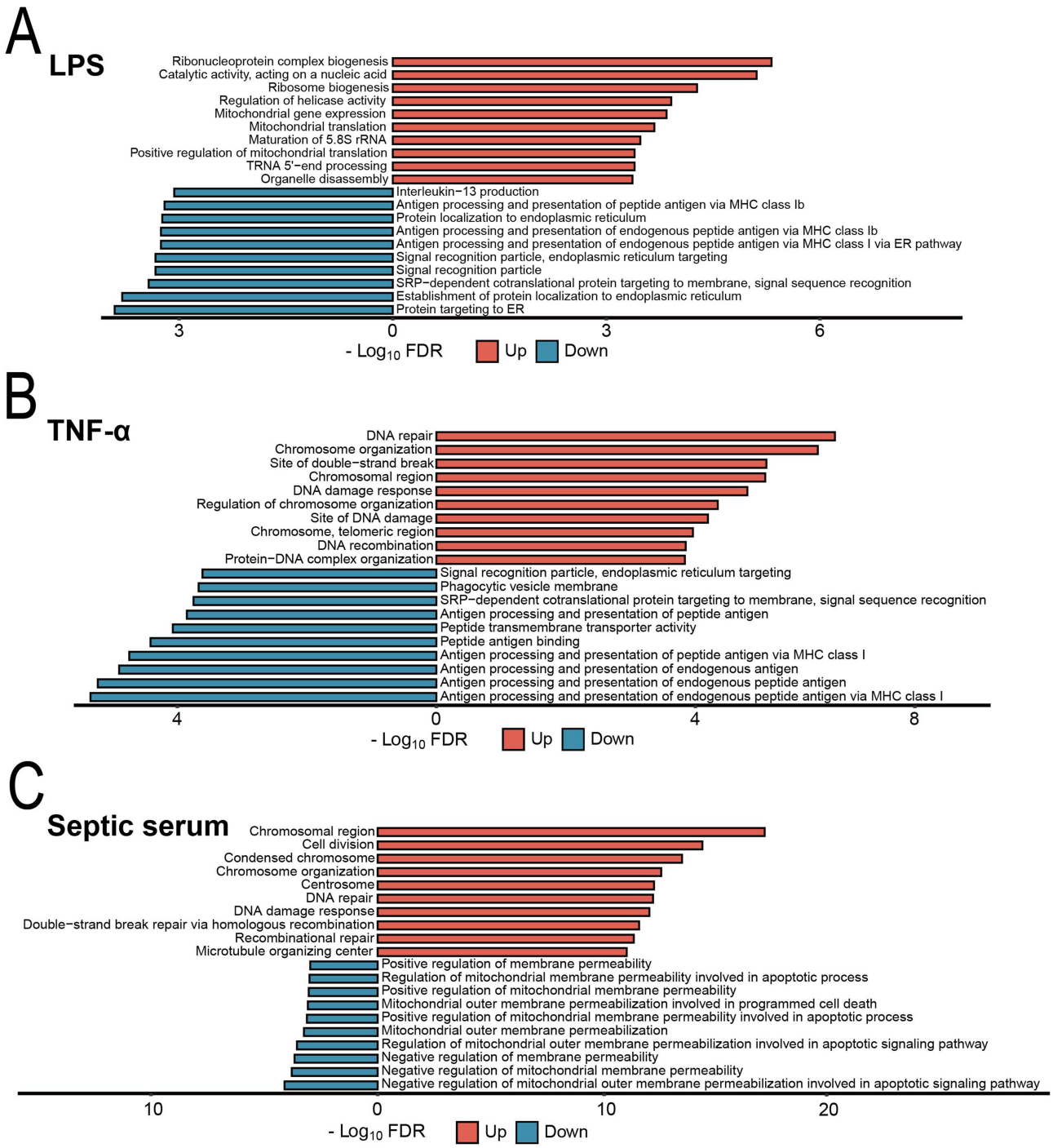

Figure 7 Gene Ontology (GO) analysis of differentially expressed genes (DEGs) in various in vitro models of sepsis-induced myocardial injury. (**A**–**C**) GO analysis of DEGs treated with LPS, TNF-α, and septic serum.

Abbreviations: LPS, Lipopolysaccharide; TNF-α, Tumor necrosis factor-α.

levels and mitochondrial dysfunction compared with LPS and TNF-α, indicating that the septic serum model is particularly suitable for investigating oxidative damage mechanisms in sepsis-induced myocardial injury.

The release of cardiac biomarkers such as BNP, CK-MB, and cTnI is commonly used to assess myocardial injury.[36–38] Our findings showed that these markers were significantly elevated in the septic serum group compared to the LPS and TNF-α groups, suggesting that the serum model more closely replicates the degree of cardiac injury observed in vivo,

https://doi.org/10.2147/JIR.S523124

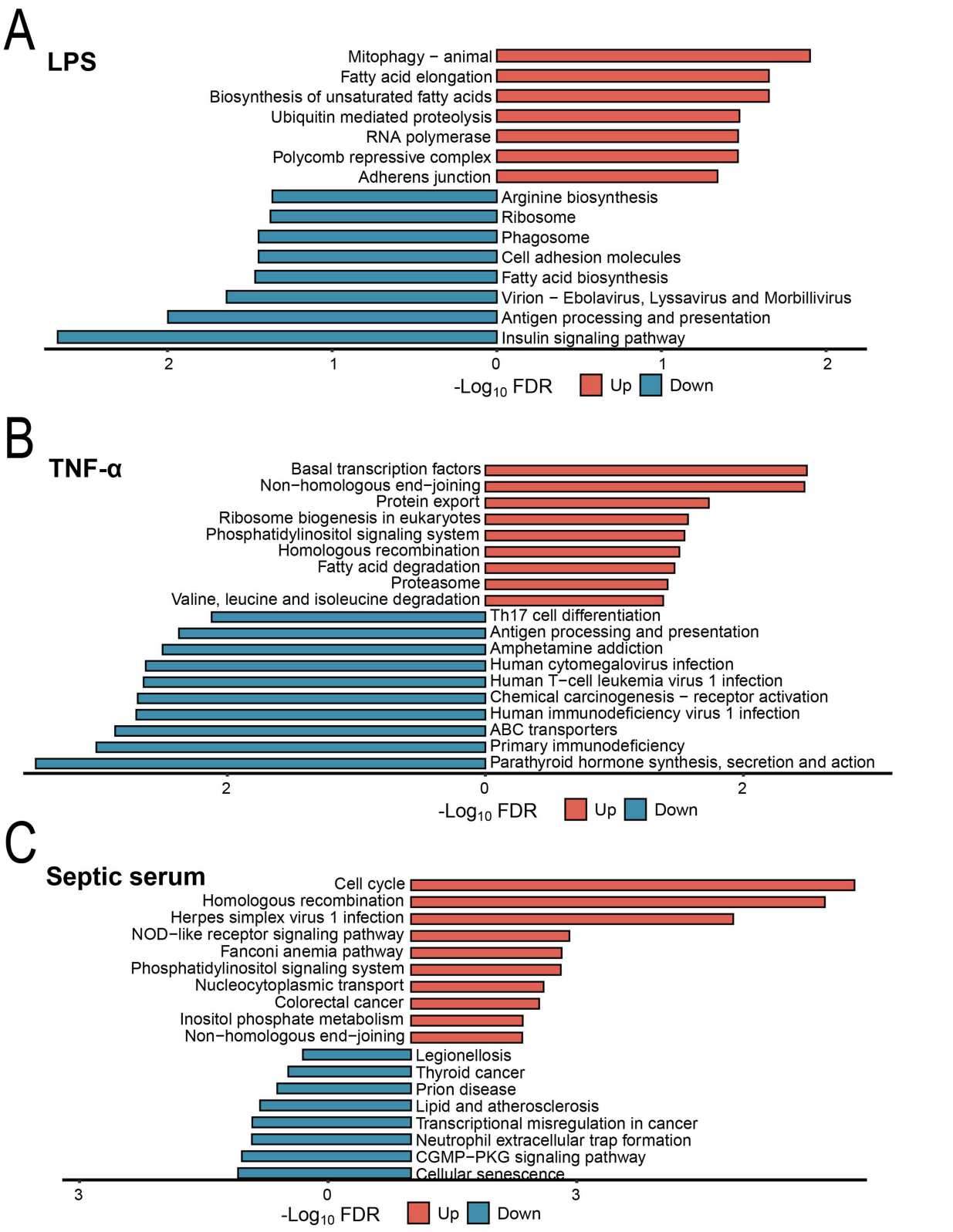

Figure 8 Kyoto Encyclopedia of Genes and Genomes (KEGG) analysis of differentially expressed genes (DEGs) in various in vitro models of sepsis-induced myocardial injury. (**A**–**C**) KEGG analysis of DEGs treated with LPS, TNF-α, and septic serum.
Abbreviations: LPS, Lipopolysaccharide; TNF-α, Tumor necrosis factor-α.

potentially due to the presence of abundant cardiotoxic factors in septic serum. However, it is important to note that increased biomarker levels reflect myocardial injury severity but do not necessarily mirror the full spectrum of sepsis-induced myocardial pathophysiology. The clinical relevance of these markers still requires further validation.[39]

In terms of cytotoxicity, septic serum induced a greater reduction in cell viability and a higher degree of apoptosis than LPS or TNF-α, likely due to the combined effects of inflammatory, oxidative, and metabolic insults. This reinforces the utility of septic serum in modeling the multifactorial nature of sepsis-induced myocardial injury. However, the extent of injury does not necessarily equate to greater physiological relevance, and model selection must be carefully considered when simulating clinical scenarios.[40,41] Ultimately, the translational value of in vitro models must be evaluated in conjunction with functional, metabolic, and electrophysiological parameters.

Transcriptomic analysis revealed that the septic serum model yielded the highest number of DEGs, which were enriched in a broader range of biological processes, suggesting a more robust transcriptional response in cardiomyocytes. GO enrichment analysis indicated that DEGs in the septic serum group were associated with "negative regulation of mitochondrial membrane permeability" and "cell division" implying the involvement of mitochondrial dysfunction, apoptotic signaling, and dysregulated cell proliferation in septic myocardial injury.[42,43] KEGG pathway analysis further revealed enrichment in pathways such as "cell cycle", "cGMP-PKG signaling", and "cellular senescence", suggesting roles for DNA damage responses, proliferative disorders, and premature cardiomyocyte senescence in the disease process.[44,45] Moreover, activation of the cGMP-PKG signaling pathway may represent a compensatory mechanism related to vasodilation and myocardial relaxation.[46,47] These data indicate that the septic serum model more accurately captures the phenotypic and molecular complexity of myocardial injury than LPS or TNF-α, which mainly triggered more limited responses related to immune activation and stress signaling.

Although LPS is widely used to induce sepsis models in vitro due to its availability and simplicity, our results suggest that LPS and TNF-α only partially mimic the multifaceted nature of clinical sepsis. In contrast, the septic serum model incorporates circulating toxins, inflammatory mediators, and metabolic dysfunctions that collectively drive myocardial injury. Nonetheless, due to its compositional complexity, future studies should focus on profiling the serum to identify key bioactive constituents responsible for cardiotoxicity. Establishing standardized serum preparation protocols will also be crucial for optimizing this model. Despite its advantages, limitations of the serum model must be acknowledged. First, the composition of septic serum may vary depending on the infection source, disease stage, and patient heterogeneity, potentially affecting reproducibility. Second, its multifactorial nature hinders attribution of specific effects to individual molecular components.

Several limitations should be considered. First, sepsis-induced myocardial injury is largely driven by cytokine release from macrophages, yet our study did not evaluate cardiomyocyte-macrophage interactions in co-culture systems. Second, functional assays assessing contractility or electrophysiological properties were not performed in the in vitro models. Third, although human cardiomyocytes were used, the transition from cellular models to clinical applicability remains limited. The in vivo complexity of sepsis cannot be fully replicated in vitro, and further validation using animal models and patient-derived cardiac tissues is needed to confirm the translational relevance of our findings.

Conclusion

The in vitro model of sepsis-induced myocardial injury established using septic serum demonstrates more pronounced pathological alterations across multiple parameters, indicating its superiority in faithfully replicating the complex pathophysiological features of sepsis-induced myocardial injury. By encompassing the multifactorial nature of sepsis, including inflammatory, oxidative, apoptotic, and metabolic components, this model provides a more physiologically relevant platform for mechanistic studies. It holds significant potential for advancing our understanding of sepsis-related cardiac dysfunction and for guiding the development of targeted therapeutic strategies.

Data Sharing Statement

Data supporting the findings of this study are available from the corresponding author upon reasonable request.

Acknowledgments

The authors would like to thank their team members for their suggestions and assistance in this study.

Author Contributions

All authors made a significant contribution to the work reported, whether that is in the conception, study design, execution, acquisition of data, analysis and interpretation, or in all these areas; took part in drafting, revising or critically reviewing the article; gave final approval of the version to be published; have agreed on the journal to which the article has been submitted; and agree to be accountable for all aspects of the work.

Funding

This work was supported by the Natural Science Foundation of Fujian Province (Grant numbers 2024J01527) and Startup Fund for Scientific Research of Fujian Medical University (Grant numbers 2023QH2032).

Disclosure

We declare that we have no conflict of interest.

References

1. Zhang Y-Y, Ning B-T. Signaling pathways and intervention therapies in sepsis. *Signal Transduct Target Ther*. 2021;6(1):407. doi:10.1038/s41392-021-00816-9
2. Rudd KE, Johnson SC, Agesa KM, et al. Global, regional, and national sepsis incidence and mortality, 1990-2017: analysis for the global burden of disease study. *Lancet*. 2020;395(10219):200–211. doi:10.1016/S0140-6736(19)32989-7
3. Hagel S, Bach F, Brenner T, et al. Effect of therapeutic drug monitoring-based dose optimization of piperacillin/tazobactam on sepsis-related organ dysfunction in patients with sepsis: a randomized controlled trial. *Intensive Care Med*. 2022;48(3):311–321. doi:10.1007/s00134-021-06609-6
4. Vieillard-Baron A, Caille V, Charron C, Belliard G, Page B, Jardin F. Actual incidence of global left ventricular hypokinesia in adult septic shock. *Crit Care Med*. 2008;36(6):1701–1706. doi:10.1097/CCM.0b013e318174db05
5. Liu S, Chong W. Roles of LncRNAs in regulating mitochondrial dysfunction in septic cardiomyopathy. *Front Immunol*. 2021;12:802085. doi:10.3389/fimmu.2021.802085
6. Zou R, Tao J, Qiu J, et al. DNA-PKcs promotes sepsis-induced multiple organ failure by triggering mitochondrial dysfunction. *J Adv Res*. 2022;41:39–48. doi:10.1016/j.jare.2022.01.014
7. Xiong X, Lu L, Wang Z, et al. Irisin attenuates sepsis-induced cardiac dysfunction by attenuating inflammation-induced pyroptosis through a mitochondrial ubiquitin ligase-dependent mechanism. *Biomed Pharmacother*. 2022;152:113199. doi:10.1016/j.biopha.2022.113199
8. Jiang C, Shi Q, Yang J, et al. Ceria nanozyme coordination with curcumin for treatment of sepsis-induced cardiac injury by inhibiting ferroptosis and inflammation. *J Adv Res*. 2024;63:159–170. doi:10.1016/j.jare.2023.10.011
9. Fujimura K, Karasawa T, Komada T, et al. NLRP3 inflammasome-driven IL-1β and IL-18 contribute to lipopolysaccharide-induced septic cardiomyopathy. *J Mol Cell Cardiol*. 2023;180:58–68. doi:10.1016/j.yjmcc.2023.05.003
10. Guo L, Shen S, Rowley JW, et al. Platelet MHC class I mediates CD8+ T-cell suppression during sepsis. *Blood*. 2021;138(5):401–416. doi:10.1182/blood.2020008958
11. Schumski A, Ortega-Gómez A, Wichapong K, et al. Endotoxinemia accelerates atherosclerosis through electrostatic charge-mediated monocyte adhesion. *Circulation*. 2021;143(3):254–266. doi:10.1161/CIRCULATIONAHA.120.046677
12. Chen L-R, Hui Y, Lu L, Wang -X-X, Zhang X-M, Wang H-X. CD1d-dependent natural killer T-cells inactivation aggravates sepsis-induced myocardial injury via T lymphocytes infiltration and IL-6 production in mice. *Int Immunopharmacol*. 2023;120:110256. doi:10.1016/j.intimp.2023.110256
13. Li Z, Yi N, Chen R, et al. miR-29b-3p protects cardiomyocytes against endotoxin-induced apoptosis and inflammatory response through targeting FOXO3A. *Cell Signal*. 2020;74:109716. doi:10.1016/j.cellsig.2020.109716
14. Chen W, Gao G, Yan M, Yu M, Shi K, Yang P. Long noncoding RNA MAPKAPK5-AS1 promoted lipopolysaccharide-induced inflammatory damage in the myocardium by sponging microRNA-124-3p/E2F3. *Mol Med*. 2021;27(1):131. doi:10.1186/s10020-021-00385-1
15. Zheng Y, Li S, Hu R, Cheng F, Zhang L. GFI-1 protects against lipopolysaccharide-induced inflammatory responses and apoptosis by inhibition of the NF-κB/TNF-α pathway in H9c2 cells. *Inflammation*. 2020;43(1):74–84. doi:10.1007/s10753-019-01095-x
16. Dhingra R, Rabinovich-Nikitin I, Rothman S, et al. Proteasomal degradation of TRAF2 mediates mitochondrial dysfunction in doxorubicin-cardiomyopathy. *Circulation*. 2022;146(12):934–954. doi:10.1161/CIRCULATIONAHA.121.058411
17. Zha W, Zhao Q, Xiao Y, et al. Mitochonic acid 5 rescues cardiomyocytes from doxorubicin-induced toxicity via repressing the TNF-α/NF-κB/NLRP3-mediated pyroptosis. *Int Immunopharmacol*. 2023;123:110736. doi:10.1016/j.intimp.2023.110736
18. Li L, Huang L, Huang C, et al. The multiomics landscape of serum exosomes during the development of sepsis. *J Adv Res*. 2022;39:203–223. doi:10.1016/j.jare.2021.11.005
19. Kato Y, Nishida O, Kuriyama N, et al. Effects of thrombomodulin in reducing lethality and suppressing neutrophil extracellular trap formation in the lungs and liver in a lipopolysaccharide-induced murine septic shock model. *Int J Mol Sci*. 2021;22(9):4933. doi:10.3390/ijms22094933
20. Song J, Park DW, Moon S, et al. Diagnostic and prognostic value of interleukin-6, pentraxin 3, and procalcitonin levels among sepsis and septic shock patients: a prospective controlled study according to the Sepsis-3 definitions. *BMC Infect Dis*. 2019;19(1):968. doi:10.1186/s12879-019-4618-7
21. Petroni RC, de Oliveira SJS, Fungaro TP, et al. Short-term obesity worsens heart inflammation and disrupts mitochondrial biogenesis and function in an experimental model of endotoxemia. *Inflammation*. 2022;45(5):1985–1999. doi:10.1007/s10753-022-01669-2
22. Zhang N, Feng H, Liao -H-H, et al. Myricetin attenuated LPS induced cardiac injury in vivo and in vitro. *Phytother Res*. 2018;32(3):459–470. doi:10.1002/ptr.5989
23. Zhu H, Zhang L, Jia H, et al. Tetrahydrocurcumin improves lipopolysaccharide-induced myocardial dysfunction by inhibiting oxidative stress and inflammation via JNK/ERK signaling pathway regulation. *Phytomedicine*. 2022;104:154283. doi:10.1016/j.phymed.2022.154283

24. Kilkenny C, Browne WJ, Cuthill IC, Emerson M, Altman DG. Improving bioscience research reporting: the ARRIVE guidelines for reporting animal research. *PLoS Biol*. 2010;8(6):e1000412. doi:10.1371/journal.pbio.1000412
25. Basso FG, Turrioni APS, Almeida LF, et al. Nutritional deprivation and LPS exposure as feasible methods for induction of cellular - A methodology to validate for vitro photobiomodulation studies. *J Photochem Photobiol B*. 2016;159:205–210. doi:10.1016/j.jphotobiol.2016.04.001
26. Yilmaz A, Reiss C, Tantawi O, et al. HMG-CoA reductase inhibitors suppress maturation of human dendritic cells: new implications for atherosclerosis. *Atherosclerosis*. 2004;172(1):85–93. doi:10.1016/j.atherosclerosis.2003.10.002
27. Bi C-F, Liu J, Yang L-S, Zhang J-F. Research progress on the mechanism of sepsis induced myocardial injury. *J Inflamm Res*. 2022;15:4275–4290. doi:10.2147/JIR.S374117
28. Jiang L, Zhang L, Yang J, et al. 1-Deoxynojirimycin attenuates septic cardiomyopathy by regulating oxidative stress, apoptosis, and inflammation via the JAK2/STAT6 signaling pathway. *Biomed Pharmacother*. 2022;155:113648. doi:10.1016/j.biopha.2022.113648
29. Liu H, Hu Q, Ren K, Wu P, Wang Y, Lv C. ALDH2 mitigates LPS-induced cardiac dysfunction, inflammation, and apoptosis through the cGAS/STING pathway. *Mol Med*. 2023;29(1):171. doi:10.1186/s10020-023-00769-5
30. Chen X-S, Cui J-R, Meng X-L, et al. Angiotensin-(1-7) ameliorates sepsis-induced cardiomyopathy by alleviating inflammatory response and mitochondrial damage through the NF-κB and MAPK pathways. *J Transl Med*. 2023;21(1):2. doi:10.1186/s12967-022-03842-5
31. Li D, Wang M, Ye J, et al. Maresin 1 alleviates the inflammatory response, reduces oxidative stress and protects against cardiac injury in LPS-induced mice. *Life Sci*. 2021;277:119467. doi:10.1016/j.lfs.2021.119467
32. Ehrman RR, Sullivan AN, Favot MJ, et al. Pathophysiology, echocardiographic evaluation, biomarker findings, and prognostic implications of septic cardiomyopathy: a review of the literature. *Crit Care*. 2018;22(1):112. doi:10.1186/s13054-018-2043-8
33. Hotchkiss RS, Karl IE. The pathophysiology and treatment of sepsis. *New Engl J Med*. 2003;348(2):138–150. doi:10.1056/NEJMra021333
34. Cimolai MC, Alvarez S, Bode C, Bugger H. Mitochondrial mechanisms in septic cardiomyopathy. *Int J Mol Sci*. 2015;16(8):17763–17778. doi:10.3390/ijms160817763
35. Lin Y, Xu Y, Zhang Z. Sepsis-Induced Myocardial Dysfunction (SIMD): the pathophysiological mechanisms and therapeutic strategies targeting mitochondria. *Inflammation*. 2020;43(4):1184–1200. doi:10.1007/s10753-020-01233-w
36. Morrow DA, Sabatine MS, Brennan M-L, et al. Concurrent evaluation of novel cardiac biomarkers in acute coronary syndrome: myeloperoxidase and soluble CD40 ligand and the risk of recurrent ischaemic events in TACTICS-TIMI 18. *Eur Heart J*. 2008;29(9):1096–1102. doi:10.1093/eurheartj/ehn071
37. Irfan A, Reichlin T, Twerenbold R, et al. Cardiomyocyte injury induced by hemodynamic cardiac stress: differential release of cardiac biomarkers. *Clin Biochem*. 2015;48(18):1225–1229. doi:10.1016/j.clinbiochem.2015.06.018
38. Mi X, Zhang Z, Cheng J, Xu Z, Zhu K, Ren Y. Cardioprotective effects of Schisantherin A against isoproterenol-induced acute myocardial infarction through amelioration of oxidative stress and inflammation via modulation of PI3K-AKT/Nrf2/ARE and TLR4/MAPK/NF-κB pathways in rats. *BMC Complement Med Ther*. 2023;23(1):277. doi:10.1186/s12906-023-04081-x
39. Pun BT, Balas MC, Barnes-Daly MA, et al. Caring for critically Ill patients with the ABCDEF bundle: results of the ICU liberation collaborative in over 15,000 adults. *Crit Care Med*. 2019;47(1):3–14. doi:10.1097/CCM.0000000000003482
40. Ryu S, Park JS, Kim HY, Kim JH. Lipid-reactive T cells in immunological disorders of the lung. *Front Immunol*. 2018;9:2205. doi:10.3389/fimmu.2018.02205
41. Monteiro M, Moreira N, Pinto J, et al. GC-MS metabolomics-based approach for the identification of a potential VOC-biomarker panel in the urine of renal cell carcinoma patients. *J Cell & Mol Med*. 2017;21(9):2092–2105. doi:10.1111/jcmm.13132
42. Itoh T, Kouzu H, Miki T, et al. Cytoprotective regulation of the mitochondrial permeability transition pore is impaired in type 2 diabetic Goto-Kakizaki rat hearts. *J Mol Cell Cardiol*. 2012;53(6):870–879. doi:10.1016/j.yjmcc.2012.10.001
43. Wang WE, Li L, Xia X, et al. Dedifferentiation, proliferation, and redifferentiation of adult mammalian cardiomyocytes after ischemic injury. *Circulation*. 2017;136(9):834–848. doi:10.1161/CIRCULATIONAHA.116.024307
44. Shan H, Li T, Zhang L, et al. Heme oxygenase-1 prevents heart against myocardial infarction by attenuating ischemic injury-induced cardiomyocytes senescence. *EBioMedicine*. 2019;39:59–68. doi:10.1016/j.ebiom.2018.11.056
45. Hu M, Zhang X, Hu C, et al. Isthmin-1 alleviates cardiac ischaemia/reperfusion injury through cGMP-PKG signalling pathway. *Cardiovasc Res*. 2024;120(9):1051–1064. doi:10.1093/cvr/cvae077
46. Krüger M, Kötter S, Grützner A, et al. Protein kinase G modulates human myocardial passive stiffness by phosphorylation of the titin springs. *Circ Res*. 2009;104(1):87–94. doi:10.1161/CIRCRESAHA.108.184408
47. Monma Y, Shindo T, Eguchi K, et al. Low-intensity pulsed ultrasound ameliorates cardiac diastolic dysfunction in mice: a possible novel therapy for heart failure with preserved left ventricular ejection fraction. *Cardiovasc Res*. 2021;117(5):1325–1338. doi:10.1093/cvr/cvaa221